Int. J. Heat Mass Transfer. Vol. 25, No. 6, pp. 807–814, 1982
Printed in Great Britain

0017-9310/82/060807-08 $03.00/0

HEAT TRANSFER FROM AN ELLIPTICAL CYLINDER MOVING THROUGH AN INFINITE PLATE APPLIED TO ELECTRON BEAM WELDING

TOSHIYUKI MIYAZAKI
The Institute of Physical and Chemical Research, Wako-shi, Saitama 351, Japan

and

WARREN H. GIEDT
Department of Mechanical Engineering, University of California, Davis, CA 95616, U.S.A.

(*Received* 17 *December* 1981)

Abstract—A general solution in elliptical coordinates for the 2-dim. steady-state temperature field around an elliptical cylinder moving with a constant velocity in an infinite plate is developed. Heat flux distributions around cylinders determined from this solution are presented for values of major to minor elliptical cylinder axes ratios of 1.0, 1.5, 2.0, 3.0 and 4.0 and for the velocity–thermal property parameter $Ub/2\alpha$ varying from 0.052 to 2.5. Total heat flow rates from cylinders were calculated by integration of these distributions. These results are then applied to the evaluation of the efficiency of full penetration electron beam welding and for the prediction of the ratio of penetration depth to power required for partial penetration electron beam welding.

NOMENCLATURE

a, major axis of elliptical cylinder;
b, minor axis of elliptical cylinder: (weld width)/2;
c, specific heat capacity of plate;
$ce(\eta, -p)$, function satisfying Mathieu equation (12);
d_b, electron beam diameter;
D, plate thickness;
$Fek(\xi, -p)$, function satisfying modified Mathieu equation (13);
h, (distance between foci of an ellipse)/2;
k, thermal conductivity of plate;
p, dimensionless velocity-thermal property parameter $= (Uh/4\alpha)^2$;
$q(\eta)$, local heat rate per unit area at η;
Q, total heat flow rate from cylinder for plate thickness D;
P, power supplied by electron beam = voltage × current;
r, radial distance in r–θ coordinate system;
T, plate temperature referenced to uniform value at infinity;
T_m, melting temperature of plate above reference value at infinity;
U, velocity of elliptical cylinder;
v, term in solution for temperature depending only on x and y;
x, y, Cartesian coordinates in plane of plate;
z, Cartesian coordinate normal to plate.

Greek symbols

α, thermal diffusivity $= k/\rho c$;
β, constant relating equations (12) and (13);
δ, ratio of ellipse major to minor axes $= a/b$;
θ, angle measured from x axis;
ρ, mass density;
ξ, η, elliptical coordinates (Fig. 2);
ϕ, function of η satisfying equation (12);
ψ, function of ξ satisfying equation (13);
ω, elliptical cylinder surface parameter $= 2p^{1/2} \cosh \xi_0$.

1. INTRODUCTION

THE TEMPERATURE distribution around and the heat flow from a cylinder moving through an infinite plate is of fundamental interest and practical importance. In contrast to the concept of a line source which involves an infinite temperature, a cylinder of finite dimension is a more realistic way of representing an actual heat source. For example, as illustrated in Fig. 1, welding with an electron beam (or a laser beam) is essentially achieved by the movement of a cavity and the surrounding molten layer through the material to be joined. The depth to width ratio is typically on the order of 10 or greater. Hence, to a first approximation, the cross section defined by the outer boundary of the molten region can be represented by a cylinder. Energy from the beam is deposited primarily on the forward surface. As incoming material is melted, it goes into a thin liquid layer on the forward half of the molten region and then flows around to the rear where it solidifies. The higher heating rates on the forward half as compared to the rear result in an elliptical-shaped solid boundary.

The solution for the temperature distribution around a circular cylinder moving with a constant velocity in an infinite plate has been derived [1], and

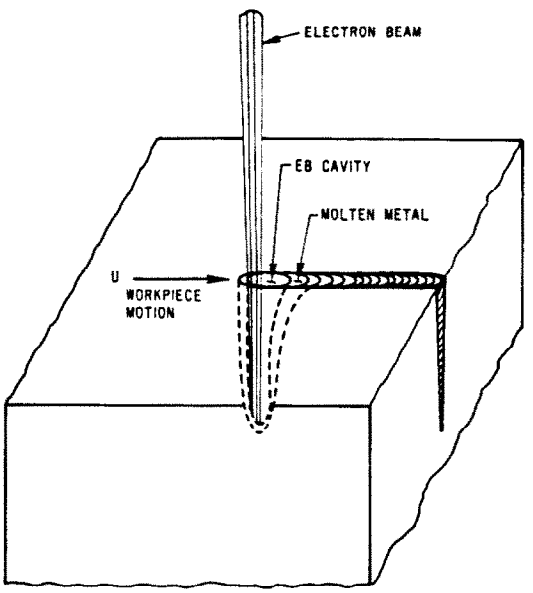

FIG. 1. The electron beam welding process.

utilized for analyzing heat transfer in electron beam welding [2]. However, the temperature field around a moving elliptical cylinder appears to be more applicable to this problem. Therefore, a formal solution for this geometry has been obtained and is described herein. Local heat transfer rate distributions and integrated heat rates have been calculated from the solution and are presented graphically. Finally, the utilization of the results to predict the relation between electron beam welding penetration and the power required is demonstrated.

2. GOVERNING DIFFERENTIAL EQUATION AND SOLUTION PROCEDURE

The problem being considered is specified schematically in Fig. 2. An elliptical-shaped cylinder of uniform cross section in z direction is moving in an infinite plate parallel to the x axis with a constant velocity. The cylinder surface is at a uniform temperature T_m so that

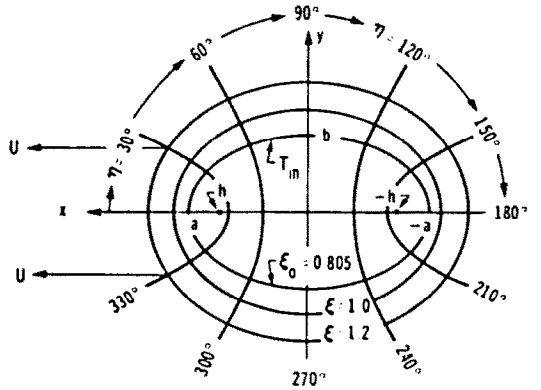

FIG. 2. Elliptical coordinates superposed on an elliptical cylinder with $\delta = a/b = 1.5$.

heat flow is only in the x and y directions. Assuming constant average thermal properties and the origin of the coordinate system fixed at the center of the cylinder, the governing differential equation and boundary conditions for the temperature T measured above the reference at infinity are then [1]

$$\frac{\partial^2 T}{\partial x^2} + \frac{\partial^2 T}{\partial y^2} + \frac{U}{\alpha}\frac{\partial T}{\partial x} = 0, \tag{1}$$

$$T = T_m \quad \text{at} \quad \frac{x^2}{a^2} + \frac{y^2}{b^2} = 1, \tag{2}$$

and

$$T \to 0 \quad \text{as} \quad x \to \pm\infty \quad \text{and} \quad y \to \pm\infty, \tag{3}$$

where α is the thermal diffusivity of the plate, U the velocity of the cylinder, T_m the temperature of the cylinder surface, and a and b the major and minor axes of the elliptical cylinder, respectively.

For problems involving a convection term in the governing differential equation (i.e. $\partial T/\partial x$), the solution can usually be expressed as the product of an exponential term and a new dependent variable v. Assuming this to be possible, $T = T_m e^{-(Ux/2\alpha)} v(x, y)$ is substituted in equation (1). This yields the following differential equation for v:

$$\frac{\partial^2 v}{\partial x^2} + \frac{\partial^2 v}{\partial y^2} = \left(\frac{U}{2\alpha}\right)^2 v. \tag{4}$$

Boundary conditions (2) and (3) then become

$$v = e^{(Ux/2\alpha)} \quad \text{at} \quad \frac{x^2}{a^2} + \frac{y^2}{b^2} = 1, \tag{5}$$

$$v \to 0 \quad \text{as} \quad x \to \pm\infty \quad \text{and} \quad y \to \pm\infty. \tag{6}$$

Because of the elliptical nature of the temperature field, it is convenient to introduce elliptical coordinates ξ and η as illustrated in Fig. 2. The relationships between ξ and η and the Cartesian coordinates x and y are normally expressed as

$$x = h \cosh \xi \cos \eta, \tag{7}$$

$$y = h \sinh \xi \sin \eta, \tag{8}$$

where $2h$ is the interfocal distance common to a family of confocal ellipses and hyperbolas. Constant values of ξ define ellipses and constant values of η define hyperbolas. With ξ and η as the independent variables, equations (4)-(6) become (ref. [3], p. 173)

$$\frac{\partial^2 v}{\partial \xi^2} + \frac{\partial^2 v}{\partial \eta^2} = 2p\,(\cosh 2\xi - \cos 2\eta)v, \tag{9}$$

$$v = e^{2p^{1/2}\cosh \xi_0 \cos \eta} \quad \text{at} \quad \xi = \xi_0, \tag{10}$$

$$v \to 0 \quad \text{as} \quad \xi \to \infty, \tag{11}$$

with $p = [(Uh)/(4\alpha)]^2$, $h \cosh \xi_0 = a$ and $h \sinh \xi_0 = b$.

Assuming there is a solution of equation (9) which can be expressed as the product of a function of η and a

function of ξ, i.e. $v = \phi(\eta) \cdot \psi(\xi)$, the functions ϕ and ψ must satisfy

$$\frac{d^2\phi}{d\eta^2} + (\beta + 2p\cos 2\eta)\phi = 0, \tag{12}$$

and

$$\frac{d^2\psi}{d\xi^2} - (\beta + 2p\cosh 2\xi)\psi = 0, \tag{13}$$

where β is the separation constant. Equation (12) is known as the Mathieu equation and equation (13) as the modified Mathieu equation. Starting at leading point of the elliptical cylinder ($x = a$, $y = 0$) and moving around the upper ξ_0 curve, η changes from 0 to π at the rear where $x = -a$ and $y = 0$. Continuing along the lower ξ_0 curve η varies from π to 2π. Since the temperature field will be symmetrical about the x axis, the solution of equation (12) must be an even function of η with period 2π. Therefore, the appropriate solution of equation (12) for the present problem is (ref. [3], p. 21)

$$\phi(\eta) = \begin{cases} ce_{2n}(\eta, -p) = (-1)^n \\ \qquad \sum_{r=0}^{r} (-1)^r A_{2r}^{(2n)} \cos 2r\eta \\ ce_{2n+1}(\eta, -p) = (-1)^n \\ \qquad \sum_{r=0}^{r} (-1)^r B_{2r+1}^{(2n+1)} \cos(2r+1)\eta, \end{cases} \tag{14}$$

where $n = 0, 1, 2, \ldots$ and the coefficients $A_{2r}^{(2n)}$ and $B_{2r+1}^{(2n+1)}$ are functions of β and p. Values of β, $A_{2r}^{(2n)}$ and $B_{2r+1}^{(2n+1)}$ for selected values of p accurate to 9 places are given in ref. [4].

The solution of equation (13) corresponding to the same values of β applicable for the solution of equation (12) [that is, equation (14)], which satisfies condition (11) is (ref. [3], p. 165)

$$\psi(\xi) = \begin{cases} Fek_{2n}(\xi, -p) = \dfrac{g'_{2n}}{\pi A_0^{(2n)}} \\ \qquad \sum_{r=0}^{r} A_{2r}^{(2n)} I_r(u_1) K_r(u_2) \\ Fek_{2n+1}(\xi, -p) = \dfrac{s'_{2n+1}}{\pi B_1^{(2n+1)}} \\ \qquad \sum_{r=0}^{r} B_{2r+1}^{(2n+1)} [I_r(u_1) K_{r+1}(u_2) \\ \qquad - I_{r+1}(u_1) K_r(u_2)], \end{cases} \tag{15}$$

where g'_{2n} and s'_{2n+1} are the constants for each n, I_r and K_r the modified Bessel functions of order r, and $u_1 = p^{1/2} e^{-\xi}$ and $u_2 = p^{1/2} e^{\xi}$.

The Mathieu functions $ce_m(\eta, -p)$ and $Fek_m(\xi, -p)$ for $m = 0, 1, 2, \ldots$ can be expressed in several forms [5], particularly $Fek_m(\xi, -p)$. The forms given in equation (15) have been found to converge more rapidly than forms not including a product of Bessel functions (ref. [3], p. 257).

Combining the results from equations (14) and (15) the product solution to equation (9) can be expressed in the following compact form

$$v = \sum_{m=0}^{r} C_m ce_m(\eta, -p) Fek_m(\xi, -p), \tag{16}$$

where the C_m's are constants determined from condition (10). From equations (10) and (16) and using the orthogonality property of $ce_m(\eta, -p)$,

$$C_m = \frac{1}{\pi Fek_m(\xi_0, -p)} \int_0^{2\pi} e^{2p^{1/2}\cosh\xi_0 \cos\eta} ce_m(\eta, -p) d\eta. \tag{17}$$

The exponential term in equation (17) can be expressed in terms of the modified Bessel function of the first kind I_r as [5]

$$e^{\omega\cos\eta} = I_0(\omega) + 2\sum_{r=1}^{r} I_r(\omega)\cos r\eta, \tag{18}$$

in which $\omega = 2p^{1/2}\cosh\xi_0$. Integration of equation (17) term by term then yields for $m = 2n$

$$C_{2n} = \frac{2(-1)^n}{Fek_{2n}(\xi_0, -p)} \sum_{r=0}^{r} (-1)^r A_{2r}^{(2n)} I_{2r}(\omega) \tag{19}$$

and for $m = 2n + 1$,

$$C_{2n+1} = \frac{2(-1)^n}{Fek_{2n+1}(\xi_0, -p)} \sum_{r=0}^{r} (-1)^r B_{2r+1}^{(2n+1)} I_{2r+1}(\omega). \tag{20}$$

Thus, the desired solution of equation (1) subject to boundary conditions (2) and (3) in elliptical coordinates is

$$\frac{T}{T_m} = e^{-2p^{1/2}\cosh\xi\cos\eta} \sum_{m=0}^{r} C_m ce_m(\eta, -p) Fek_m(\xi, -p). \tag{21}$$

Circular cylinder solution

When the minor axis b of an ellipse approaches the value of the major axis a or vice versa, the ellipse approaches a circle. Hence, equation (21) should reduce to the solution for the temperature distribution around a circular cylinder. To show this note that when $a \to b$ or $b \to a$, since $h^2 = a^2 - b^2$, this means that $h \to 0$ and $p \to 0$. The confocal hyperbolas then become radii of the circle defining an angle θ. In this case (see ref. [3], p. 367)

$$ce_m(\eta, -p) = \cos m\theta \quad (m \geq 1),$$

$$ce_0(\eta, -p) = 1/\sqrt{2}.$$

Also when an ellipse with major axis r is made to approach a circle with radius r, $h \to 0$ and $\xi \to \infty$ such

that $h \cosh \xi \to r$, (i.e. $1/2\, he^{\xi} \to r$). It can then be shown that

$$Fek_{2n}(\xi, -p) = \frac{g'_{2n}}{\pi} K_{2n}\left(\frac{Ur}{2\alpha}\right),$$

and

$$Fek_{2n+1}(\xi, -p) = \frac{s'_{2n+1}}{\pi} K_{2n+1}\left(\frac{Ur}{2\alpha}\right).$$

Equation (21) then becomes

$$\frac{T}{T_m} = e^{-\frac{Ur}{2\alpha}\cos\theta} \sum_{m=0}^{\infty} \varepsilon_m I_m\left(\frac{Ur_0}{2\alpha}\right) \frac{K_m\left(\frac{Ur}{2\alpha}\right)}{K_m\left(\frac{Ur_0}{2\alpha}\right)} \cos m\theta, \quad (22)$$

where θ is now the angle in an r–θ coordinate system, r_0 the radius of the circular cylinder, and $\varepsilon_0 = 1$, $\varepsilon_1 = \varepsilon_2 = \ldots = 2$. The solution given by equation (22) is the same as that derived in ref. [1] for a circular cylinder.

3. HEAT TRANSFER FROM AN ELLIPTICAL CYLINDER

The local heat flux $q(\eta)$ from the elliptical cylinder surface at a temperature T_m into the surrounding solid is given by

$$q(\eta) = -k \left.\frac{\partial T}{\partial n}\right|_{\xi_0}, \quad (23)$$

where k is the thermal conductivity of the solid and n denotes the direction normal to the surface. In terms of ξ and η the differential $dn = h(\cosh^2\xi - \cos^2\eta)^{1/2}\, d\xi$. Substituting this relation and introducing T_m and $h^2 = a^2 - b^2$ leads to the following nondimensional form for the local heat flux:

$$\frac{q(\eta)b}{kT_m} = \frac{-1}{[(\delta^2 - 1)(\cosh^2\xi_0 - \cos^2\eta)]^{1/2}} \left.\frac{\partial(T/T_m)}{\partial\xi}\right|_{\xi_0}, \quad (24)$$

where $\delta = a/b$, the ratio of the major to minor axes of the ellipse. The equation for $[\partial(T/T_m)/\partial\xi]_{\xi_0}$ is given by

$$\left.\frac{\partial(T/T_m)}{\partial\xi}\right|_{\xi_0} = -2p^{1/2}\sinh\xi_0\cos\eta + e^{-\omega\cos\eta} \sum_{m=0}^{\infty} C_m ce_m(\eta, -p) \left.\frac{dFek_m(\xi, -p)}{d\xi}\right|_{\xi_0}, \quad (25)$$

where for $m = 2n$

$$\frac{dFek_{2n}(\xi, -p)}{d\xi} = -\frac{g'_{2n}}{\pi A_0^{(2n)}}\left[A_0^{(2n)}\{u_1K_0(u_2)I_1(u_1) + u_2I_0(u_1)K_1(u_2)\} + \sum_{r=1}^{\infty} A_{2r}^{(2n)} \cdot \left\{\frac{u_1}{2}K_r(u_2)\cdot[I_{r-1}(u_1) + I_{r+1}(u_2)] + \frac{u_2}{2}I_r(u_1)\cdot[K_{r-1}(u_2) + K_{r+1}(u_2)]\right\}\right] \quad (26)$$

and for $m = 2n + 1$

$$\frac{dFek_{2n+1}(\xi, -p)}{d\xi} = -\frac{s'_{2n+1}}{\pi B_1^{(2n+1)}}\left[B_1^{(2n+1)}\left\{u_1K_1(u_2)I_1(u_1) + \frac{u_2}{2}I_0(u_1)\cdot[K_0(u_2) + K_2(u_2)]\right\} + \sum_{r=1}^{\infty} B_{2r+1}^{(2n+1)}\left\{\frac{u_1}{2}K_{r+1}(u_2)\cdot[I_{r-1}(u_1) + I_{r+1}(u_1)] + \frac{u_2}{2}I_r(u_1)\cdot[K_r(u_2) + K_{r+2}(u_2)]\right\}\right]. \quad (27)$$

The total heat flow rate Q from the cylinder for a plate thickness D is given by

$$\frac{Q}{kT_mD} = -2\int_0^{\pi} \left.\frac{\partial(T/T_m)}{\partial\xi}\right|_{\xi_0} d\eta. \quad (28)$$

The RHS of equation (28) is a function of p and ξ_0, which can be expressed in terms of the commonly used velocity-diffusivity parameter $Ub/2\alpha$ and the ellipse axis ratio $\delta = a/b = \operatorname{ctnh}\xi_0$. That is,

$$\frac{Q}{kT_mD} = f\left(\frac{Ub}{2\alpha}, \delta\right). \quad (29)$$

Values for (Q/kT_mD) were obtained by numerical integration of the local heat flux given by equation (24).

4. RESULTS

Examples of heat flux distributions calculated from equation (24) for values of $\delta = 1.5, 2.0, 3.0$ and 4.0 are shown in Figs. 3–6. For each case distributions were computed for values of $p = (Uh/4\alpha)^2$ of 0.01, 0.1, 0.25, 0.5, 1.0 and 2.0. However, the curves have been labeled according to the values of $Ub/2\alpha = (4p/(\delta^2 - 1))^{1/2}$ because of the common use of this parameter. Heat flux distributions for the limiting case of the circular cylinder are presented in Fig. 7.

Comparison of the heat flux for $\theta \sim 0$ with increase of $Ub/2\alpha$ for different values of $\delta = a/b$ shows that the increase is greater for cylinders with lower values of δ. That is, the heat flux in the region of $\theta \sim 0$ increases more rapidly with $Ub/2\alpha$ as the elliptical cylinders become more blunt. Thus the highest rate of increase occurs with a circular cylinder as shown in Fig. 7.

However, if the heat fluxes at $\theta = 0$ for the same value of $Ub/2\alpha$ but different values of δ are compared, it is seen that $q(0)$ increases with increasing δ. The reason for this is that the less blunt the forward surface of the cylinder, the heat can flow more rapidly toward the side (i.e. toward increasing values of θ). Because of this

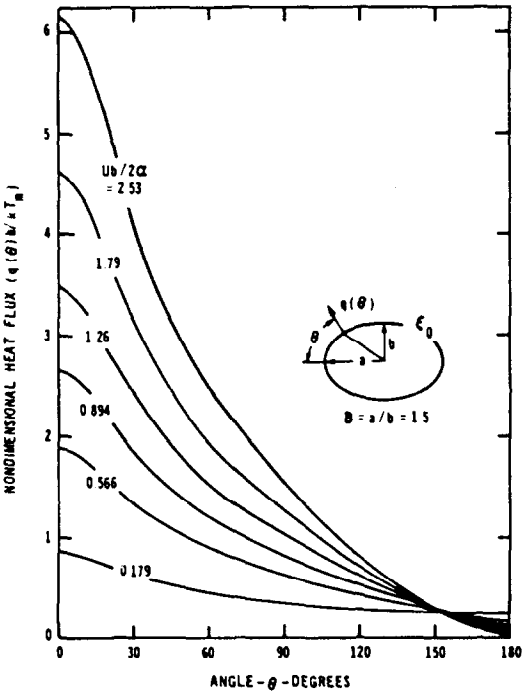

FIG. 3. Heat flux distributions around an elliptical cylinder (δ = 1.5) moving in an infinite plate.

a higher flux is required at $\theta = 0$ for equivalent cylinder velocities as δ increases.

The general trend of the local heat flux $q(\theta)$ can be seen in Figs. 3–7 to decrease much more rapidly with θ for higher values of δ. This result is of course due to the fact that the heat flow becomes almost 1-dim. toward the side as an ellipse becomes elongated. Note that for $\delta = 4$ in Fig. 6 the region between $\theta \sim 30$–$150°$ is relatively constant.

Results for the total heat flow rate from elliptical

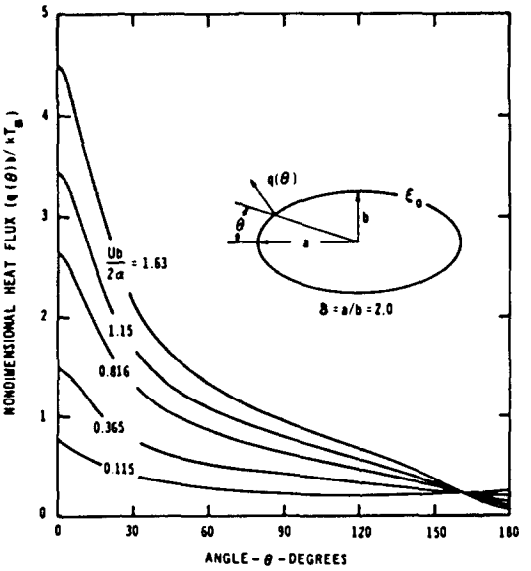

FIG. 4. Heat flux distributions around an elliptical cylinder (δ = 2.0) moving in an infinite plate.

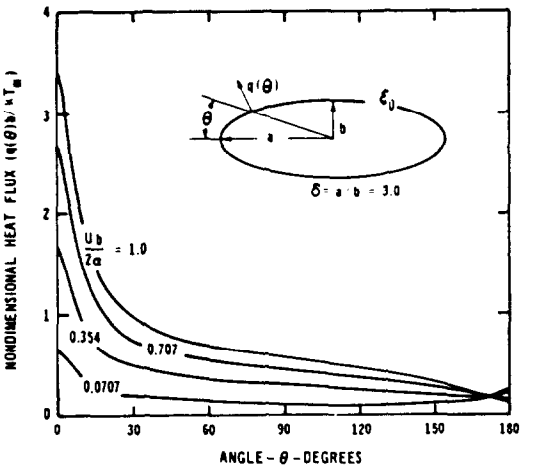

FIG. 5. Heat flux distributions around an elliptical cylinder (δ = 3.0) moving through an infinite plate.

cylinders with δ = 1.0, 1.5, 2.0, 3.0 and 4.0 are shown in Fig. 8. For a representative value of $Ub/2\alpha = 1.0$ the total heat flux can be seen to increase by approx. 50% as the cylinder is varied from circular to elliptical with $\delta = 4.0$. In view of the substantial increase in surface area (by about 2.7 from a circle to ellipse with $\delta = 4.0$) it is surprising that the increase is not greater. The explanation lies in the very rapid decrease of the local heat flux around elliptical cylinders with large values of δ.

5. APPLICATION OF RESULTS TO ELECTRON BEAM WELDING

The solution presented in this paper provides an appropriate boundary condition for analysis of partial and full penetration electron beam welding and can be used for specifying the boundary condition for analysis of the heat flow in the molten layer. The application for determination of power absorption in full penetration and of penetration depth in partial penetration welding will be discussed in the following sections.

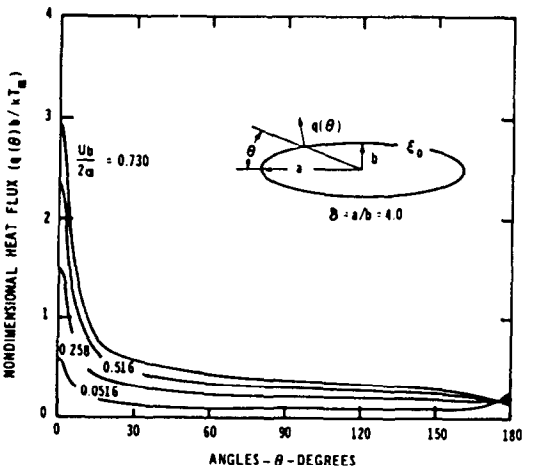

FIG. 6. Heat flux distributions around an elliptical cylinder (δ = 4.0) moving through an infinite plate.

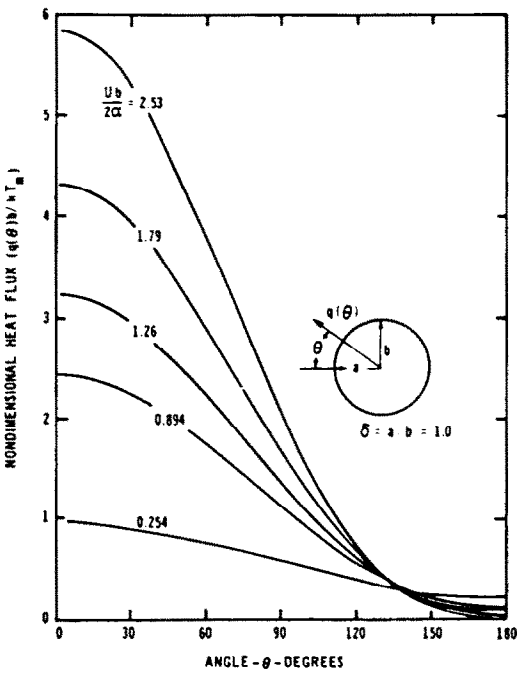

FIG. 7. Heat flux distributions around a circular cylinder moving through an infinite plate.

Full penetration welding

When a thin plate is welded, electrons can penetrate through to the rear surface of the plate and the cavity can become a channel, in which case part of the electron beam power passes through the plate. This is called full penetration and can be modeled as suggested in Fig. 9. Noting that the solid boundary of the weld region decreases linearly from the upper to the lower surface and assuming that the total heat flow rate at any horizontal plane is approximately expressed by equation (29), the power P absorbed in a plate of thickness D can be determined from

$$P = kT_m \int_0^D f\left(\frac{Uy}{2\alpha}, \delta\right) dz, \tag{30}$$

where $2y$ is the weld width at the depth z and $y = b$ at $z = 0$ and $y = b_0$ at $z = D$. For constant α and U, this can be written in the following nondimensional form:

$$\frac{P}{kT_m D} = \frac{1}{\dfrac{U(b-b_0)}{2\alpha}} \int_{Ub_0/2\alpha}^{Ub/2\alpha} f(w, \delta)\, dw \tag{31}$$

in which $w = Uy/2\alpha$ with y varying from b_0 to b. When the width of the welded region $2b$ is constant (i.e. $b_0 = b$), which essentially occurs when a thin plate is welded by a high power density electron beam, the nondimensional power is simply

$$\frac{P}{kT_m D} = f\left(\frac{Ub}{2\alpha}, \delta\right). \tag{32}$$

Some experimental results are given in Table 1. In this table, the efficiency represents the ratio of the power absorbed in the plate to the total power.

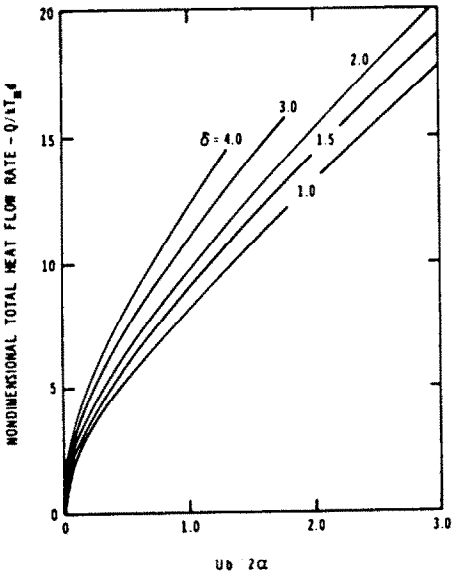

FIG. 8. Total heat flow rate from elliptical cylinders moving through an infinite plate.

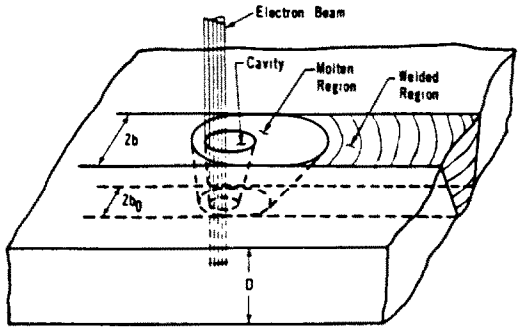

FIG. 9. Electron beam welding full penetration model.

Partial penetration welding

Determining the welding conditions (beam power, focus current, and speed) to achieve a specified penetration depth in a particular material is a problem

Table 1. Efficiency in full penetration welding in 304 stainless steel

	(1)	(2)
Power (kW)	1.75 kW, (25 kV, 70 mA)	2.0 kW, (25 kV, 80 mA)
Speed, U (mm s^{-1})	5	5
Thickness, D (mm)	2.8	1.6
Weld width, $2b$ (mm)	3.3 2.3	2.3 2.3
Efficiency	0.4	0.2

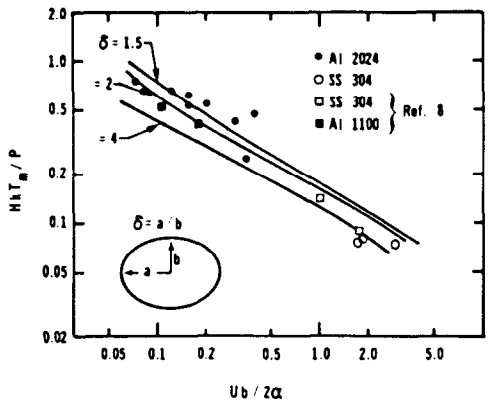

FIG. 10. Partial penetration depth to power ratio variation with $Ub/2\alpha$.

which has received considerable attention. A number of different analyses and correlations have been reported [2, 6] and in general all show reasonable agreement with experimental data. Predicted results are usually presented in terms of a nondimensional parameter incorporating penetration depth and power as a function of the welding speed–thermal property parameter $Ud_b/2\alpha$ in which d_b is the diameter of the focused electron beam. Unfortunately, it is not exactly clear as to how d_b should be defined. Also measurements of beam intensity distributions are difficult and impractical to make. Because of questions regarding the value of values of beam diameter used, definitive comparisons of measurements of different investigators are difficult to make.

For an electron beam entering a cavity the fraction reflected is small, and losses due to radiation and metal evaporation can be shown to be negligible. Hence, all the energy deposited in a welding cavity will be eventually lost by conduction to the surrounding solid because the energy which goes into melting and raising the temperature of the liquid formed is returned in the rear part of the molten region during solidification.

The actual cross section of the weld region in partial penetration welding is triangular in shape. In this case, with $b_0 \to 0$ in equation (31), D becomes the penetration depth H in partial penetration welding. Hence,

$$\frac{kT_mH}{P} = \frac{Ub/2\alpha}{\int_0^{Ub/2\alpha} f(w, \delta)\,dw} \tag{33}$$

where w denotes $Uy/2\alpha$ with y varying from 0 to b. Relationships between the value of the RHS of equation (33) and the value of $Ub/2\alpha$ are shown in Fig. 10 for $\delta = 1.5$, 2.0 and 4.0. Applicable values of δ are expected to depend on material and welding conditions. As can be observed, however, the effect of δ is not large and a mean curve corresponding to $\delta \sim 2.0$ may be adequate for general use. Comparison of limited penetration measurements for which normal cross sections were available show acceptable agreement with predictions. Although results for aluminum tend to fall around the $\delta = 1.5$ line and those for stainless steel around $\delta = 4.0$, more data are needed to establish the applicability of the proposed model. The new approach to predicting penetration depth leading to Fig. 10 has a good theoretical foundation, however, and introduces the use of the desired weld region geometry instead of the electron beam diameter. The latter factor is considered to be of significant practical importance.

Acknowledgements—The support of the National Science Foundation under Grant No. CME-7911288 is gratefully acknowledged. The authors also express appreciation to Mr. Bruce Bolden for his assistance.

REFERENCES

1. H. S. Carslaw and J. C. Jaeger, *Conduction of Heat in Solids* (2nd edn.), p. 390. Clarendon, Oxford (1962).
2. H. Tong and W. H. Giedt, Depth of penetration during electron beam welding, *Trans. Am. Soc. Mech. Engrs.* Series C, *J. Heat Transfer* 93, 155 (1971).
3. N. W. McLachlan, *Theory and Application of Mathieu Functions* (1st edn.). Clarendon, Oxford (1951).
4. A. N. Lowan, *Tables Relating to Mathieu Functions* (Applied Mathematics, Series 59), p. 41. National Bureau of Standards (1967).
5. A. Gray and T. M. Macrobert, *Bessel Functions* (2nd edn.), p. 36. Macmillan, London (1952).
6. M. H. Hablanian, A correlation of welding variables, *Proc. 5th Electron and Ion Beam Symp.*, Boston (edited by J. R. Moreley), p. 262. Alloyd Electronics, Cambridge, Mass., U.S.A. (1963).
7. S. M. Shintaku, Temperature distributions in electron beam welding cavities, M.S. Thesis, University of California, Davis (1976).

APPENDIX

Range of calculations

Calculations of the heat flux distributions from equation (24) involved evaluation of

$$e^{-\omega\cos\eta}\sum_{m=0}^{s} C_m ce_m(\eta, -p)\left.\frac{dFek_m(\xi, -p)}{d\xi}\right|_{\xi_0}, \tag{A1}$$

in which $\omega = 2p^{1/2}\cosh\xi_0$ and $p = (Uh/4\alpha)^2$. For a given ellipse and plate material with diffusivity α, ω is a measure of elliptical cylinder velocity. As η varies from 0 to π, the quantity $(-\omega\cos\eta)$ varies from $-\omega$ to $+\omega$. This causes the exponential term multiplying the summation in the above equation to change from a small to a relatively large number. The importance of this change can be illustrated by showing its effect on the temperature at the cylinder boundary where $\xi = \xi_0$ and $T = T_m$. Equation (21) then becomes

$$\left.\frac{T}{T_m}\right|_{\xi_0} = 1.0 = e^{-\omega\cos\eta}\sum_{m=0}^{s} C_m ce_m(\eta, -p)\,Fek_m(\xi_0, -p). \tag{A2}$$

In making calculations a value of p was first selected and the RHS of equation (A2) was evaluated for several values of ξ_0 (which depends on $\delta = a/b$). To obtain consistent heat flux values it was found that the values of the RHS of equation (A2) for all values of η had to be within $\pm 0.01\%$ of unity. Calculations were carried out with a PDP 11/34 computer using single precision accuracy (7 significant places). With this level of precision it was possible to satisfy the 0.01% requirement for $0 \le \eta \le \pi$ for values of ω up to approx. 5.0. This places a limit on values of p and the axis ratio δ (which

determines ξ_0). To show this consider the case of $p = 5, \delta = 1.5$ ($\xi_0 = 0.8047190$) for which $\omega = 6.0$. At $\eta = \pi, e^{-\omega\cos\eta} = 4.034289 \times 10^2$. The summation by which this is multiplied (evaluated to 16 terms) is

$$\sum_{m=0}^{15} C_m ce_m(\pi, -5) Fek_m(0.8047190, -5)$$

$$= 1.821003 \times 10^2 - 1.825812 \times 10^2 + 1.222649 \times 10^1 - 1.538394 \times 10^1 + \ldots + 1.231942 \times 10^{-5} - 2.011957 \times 10^{-7}$$

$$= (1.821003 \times 10^2 + 1.222649 \times 10^1 + \ldots + 1.231942 \times 10^{-5}) - (1.825812 \times 10^2 + 1.538394 \times 10^1 + \ldots + 2.011959 \times 10^{-7})$$

$$= 2.441407 \times 10^{-3}.$$

The resulting value for $(T/T_m)_{\xi_0}$ yields a value of 0.9849340. Using more terms does not definitely increase the accuracy because of round-off errors in the terms already included. Thus to extend the range of the calculations over all η higher precision in the individual terms of the series would be required. On the other hand, in the region around $\eta = 0$,

$$\sum_{m=0}^{15} C_m ce_m(0, -5) Fek_m(0.8047190, -5) = 4.034289 \times 10^2,$$

so that the temperature ratio is 0.9999996. Thus over the forward part of a cylinder acceptable results can be obtained for larger values of ω. Fortunately the range of values of $\omega \cos\eta$ for which results were obtained correspond to values of practical interest for the parameters $Ub/2\alpha$ and δ.

TRANSFERT THERMIQUE A PARTIR D'UN CYLINDRE ELLIPTIQUE EN DEPLACEMENT TRAVERS UNE PLAQUE INFINIE EN APPLICATION DU SOUDAGE PAR FAISCEAU D'ELECTRONS

Résumé—On développe une solution générale en coordonnées elliptiques pour le champ de température bidimensionnel permanent autour d'un cylindre elliptique se déplaçant à vitesse constante dans une plaque infinie. Les distributions de flux thermique autour des cylindres sont présentées pour des valeurs du rapport d'axes du cylindre de 1,0–1,5–2,0–3,0 et 4,0 et pour 2,5. Les flux thermiques totaux sont calculés par intégration de leurs distributions. Ces calculs sont alors appliqués à l'évaluation de l'efficacité du soudage par faisceau d'électrons à pleine pénétration et à la prévision du rapport de la profondeur de pénétration à la puissance nécessaire pour une pénétration partielle.

WÄRMEÜBERGANG EINES DURCH EINE UNENDLICHE PLATTE BEWEGTEN ELLIPTISCHEN ZYLINDERS, ANGEWANDT AUF ELEKTRONENSTRAHL-SCHWEISSUNG

Zusammenfassung—Eine allgemeine Lösung in elliptischen Koordinaten für das zweidimensionale stationäre Temperaturfeld um einen elliptischen Zylinder, der sich konstanter Geschwindigkeit in einer unendlichen Platte bewegt, wurde entwickelt. Aus dieser Lösung berechnete Wärmestromdichte-Verteilungen um den Zylinder werden für Verhältniswerte von Haupt- zu Nebenachse des elliptischen Zylinders von 1,0; 1,5; 2,0; 3,0 und 4,0, und für Werte des Parameters aus Geschwindigkeit und thermischen Eigenschaften $Ub/2\alpha$ zwischen 0,052 und 2,5 angegeben. Der Gesamtwärmestrom des Zylinders wurde durch Integration dieser Verteilungen berechnet. Die Ergebnisse werden zur Abschätzung der Güte von Elektronenstrahl-Schweißungen bei voller Eindringtiefe angewandt und zur Voraussage des Verhältnisses von Eindringtiefe zu erforderlicher Leistung bei Elektronenstrahl-Schweißung mit teilweisem Eindringen.

ИССЛЕДОВАНИЕ ТЕПЛОПЕРЕНОСА ЭЛЛИПТИЧЕСКОГО ЦИЛИНДРА, ПЕРЕМЕЩАЮЩЕГОСЯ СКВОЗЬ БЕСКОНЕЧНУЮ ПЛАСТИНУ, В ПРИЛОЖЕНИИ К СВАРКЕ ЭЛЕКТРОННЫМ ПУЧКОМ

Аннотация — В эллиптических координатах получено общее решение для двумерного стационарного температурного поля в окрестности эллиптического цилиндра, движущегося с постоянной скоростью сквозь бесконечную пластину. По этим решениям найдены распределения теплового потока вокруг цилиндров для отношений эллиптических осей, равных 1,0; 1,5; 2,0; 3,0 и 4,0 и для диапазона $Ub/2\alpha$ (скорость — тепловой параметр) от 0,052 до 2,5. Суммарные тепловые потоки рассчитывались интегрированием полученных распределений. Результаты затем использовались для оценки эффективности сварки электронным пучком, проникающим на всю глубину материала, и для расчета отношения глубины проникновения пучка к мощности, требуемой при сварке с частичным проникновением электронного пучка.